

DIGITAL IMAGE PROCESSING AND STEREOSCOPIC MEASUREMENT
OF A CONVERGENT PAIR OF IMAGES

Chuji Mori and Mikio Hirokane
Dept. of Civil Eng., Faculty of Eng., Okayama Univ.
Japan
Comission V

ABSTRACT

The following two subjects are described in this report. As an example of flexibility of digital photogrammetric system, stereoscopic measurements of a pair of strongly convergent images were accomplished. As to a measuring accuracy, fairly good results were attained by use of a CCD camera which provide 3000 x 2000 pixels with the aid of a scanning mechanism.

1. Introduction

Technology related to digital image acquisition and processing comes into wide use. Many of universities in Japan are provided with a large scale general-purpose computer and digital image processing system. Considering such situation, the authors investigated feasibilities of stereoscopic measurement of a pair of convergent images by use of an image processing system currently used. As a CCD camera with high resolving power (2000 x 3000 pixels) were used in this investigation, the accuracy tests of this camera were also carried out.

The results are as follows : (1) Stereoscopic measurement could be done by viewing an image pair represented on a screen of display unit with the aid of a stereoscope, (2) the accuracy of the camera were reasonably good enough.

2. Camera and Image Processing System

2-1 Camera for Digital Imaging

Image acquisition was performed by a CCD camera with a high resolving power made by Ikegami Tsushinki Co.,Ltd., named PIC-2350A. 6×10^6 pixel data are recorded by this camera. Such huge data can be obtained by scanning a focal plane of a camera with a line sensor which is made from a CCD array with 2,000 pixels as shown in Fig.1 and Tabel 1.

This scanning mechanism probably results in a fault, namely it may lead to non-uniform and unstable movement of the sensor. Therefore positional stability of the pixels was investigated. From the test results shown in Table 2, it is found that the fault does not produce so severe errors.

2-2 Digital Image Data Acquisition and Recording

The hardware system is shown in Fig.2. Basic operations for taking a image are practiced through a control unit by use of a operation board. It takes 6 seconds to take an image of a full scene or to record a digital image data to a 6 MB buffer memory. Special or complicated operations and the transfer of

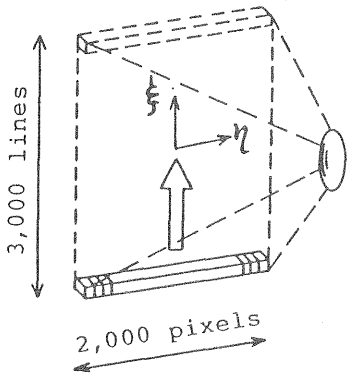


Fig.1 Camera with a line sensor

Table 1 Technical data of a camera PIC-2350A

Sensor	Charge coupled device
Pixel pitch	13 μm
Image size	2,000 x 3,000 pixels (26x39mm)
Image signal	Black and white, digitized to 8 bit
Lens	SEKOR C 45mm/2.8 N made by Mamiya Camera Co., Ltd.

the recorded data are performed by a personal computer.

Digital image data are finally transferred to a memory of a computer system, NEAC 1000 in Okayama University, by off-line process in order to use an image processing system for general purpose. A color image display in this system has a screen of 512x512 pixels and a cursor.

Table 2 Unstability of pixel position caused by scan of a focal plane. σ_{ξ} and σ_{η} are the standard errors of a position of a pixel obtained on the image plane.

Test No.	1	2	3	4
σ_{ξ} (μm)	1.7	1.5	4.3	4.8
σ_{η} (μm)	1.5	1.9	1.7	0.7

3. Measurements of Image Coordinates

3-1 Coordinate measurements of Targets

Circular targets were placed on the control points for signaling. The diameter of a central mark of a target was 2~3 times as large as pixel pitch (26 x 39 μm) on an original image. For measurement of coordinates of a center of a target, an original image was enlarged by 10 times and represented on the screen of a display unit. In other words, one pixel of an original image was replaced by 10x10 pixels in the processing

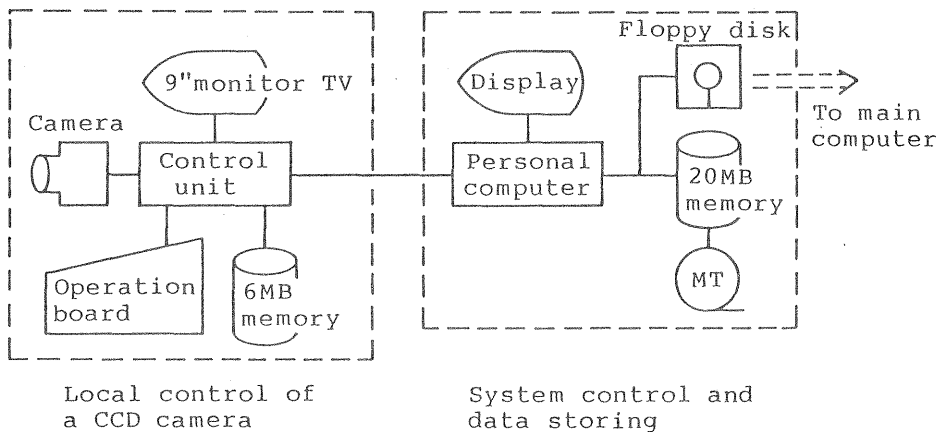


Fig.2 Configuration of image acquisition system

system. Both methods of interpolation, bi-linear and cubic convolution method, were applied in the digital image enlargement. Coordinates of a center of a target could easily be found out on the enlarged image represented in the screen by use of the cursor.

Observation error of coordinates of a center of a target was fairly small. The standard error of that observation was about 0.43 pixel pitch on the screen, or 0.043 pixel pitch (0.55 μm on the original image).

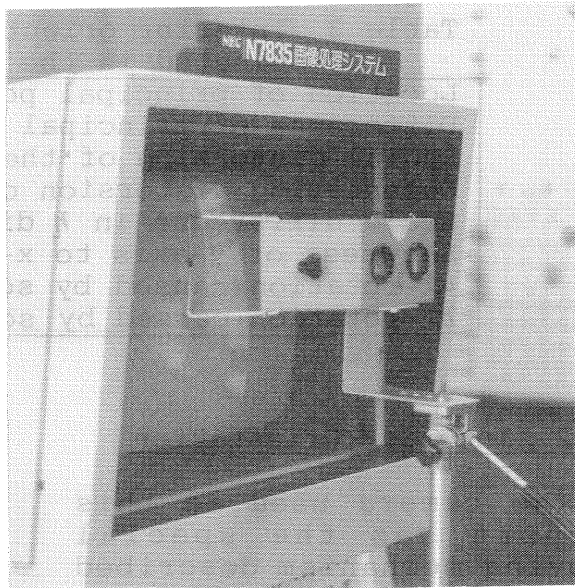


Fig.3 Arrangement for stereoscopic viewing

3-2 Stereoscopic measurement

For viewing a overlapping area of two images stereoscopically, the left and right images of that area were displayed in the left and right half parts of the screen respectively. A mirror stereoscope was used for stereoscopic viewing of the displayed image pair instead of the anaglyphic method.¹⁾²⁾ Fig.3 shows the display unit and a mirror stereoscope. In practicing this viewing method, we found that only small part of a full scene could be represented because the image size, or pixel number, of the screen was too small as compared with the one of the camera. This fact results in a defect described in the Section 6.

For the purpose of getting an exact stereoscopic perception, a y-parallax-free image pair, or a rectified image pair, should be represented. We can easily produce that image pair by digital image processing techniques even though a pair is convergent images or other unusual images after their relative orientation elements have been known. This fact is an excellent advantage in the method presented here.

4. Camera Calibration

4-1 Test Field and Method of Camera Calibration

A Test field is constructed by placing targets on the walls of a building. More than 45 targets are placed within the extent of 30 m width, 11 m height and 14 m depth(distance).

Camera calibration was carried out at each single image by applying the well-known colinearity condition :

$$\xi - \Delta\xi = -C \frac{l_1(X-X_0) + m_1(Y-Y_0) + n_1(Z-Z_0)}{l_3(X-X_0) + m_3(Y-Y_0) + n_3(Z-Z_0)}$$

$$\eta - \Delta\eta = -C \frac{l_2(X-X_0) + m_2(Y-Y_0) + n_2(Z-Z_0)}{l_3(X-X_0) + m_3(Y-Y_0) + n_3(Z-Z_0)}$$

in which $\Delta\xi$ and $\Delta\eta$ are distortions of an image.

Table 3 Interior orientation elements
selected in the first stage

Location of principal point :	ξ_0, η_0
Difference of principal distance :	C
Radial distortion of the lens :	A_1 and A_2
Decentering distortion of the lens :	B_1 and B_2
Scale difference in η direction :	λ
Skewness of y-axis to x-axis ^{*)} :	α
ω -rotation caused by scanning ^{*)} :	θ_1
π -rotation caused by scanning ^{*)} :	θ_3

4-2 Interior Orientation Elements

The camera used in this report has the special moving mechanism described above. In order to correct the image deformation effectively and sufficiently, the geometrical properties of the special mechanism were considered, and 8 interior orientation elements were selected at first. These elements consist of 11 parameters as shown in Table 3. The distortions $\Delta\xi$ and $\Delta\eta$ of an image at a location ξ, η caused by the parameters are given by the following equations, under the assumption that each parameter is very small.

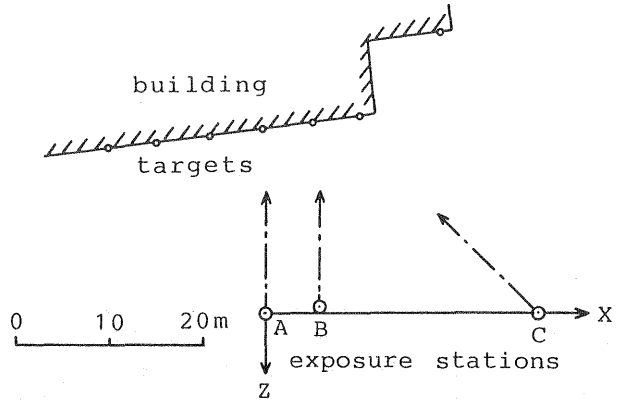


Fig.4 Plan of the test field

The distortions $\Delta\xi$ and $\Delta\eta$ of an image at a location ξ, η caused by the parameters are given by the following equations, under the assumption that each parameter is very small.

$$\Delta\xi = \xi_0 + \alpha\xi - \frac{\theta_1}{C} \xi^2 \eta + \theta_3 \xi \eta + A_1 \xi r^2 + A_2 \xi r^4 + B_1 (3\xi^2 + \eta^2) + 2B_2 \xi \eta$$

$$\Delta\eta = \eta_0 - \lambda\eta - \frac{\theta_1}{C} \left(1 + \frac{\eta^2}{C^2}\right) \xi + A_1 \eta r^2 + A_2 \eta r^4 + 2B_1 \xi \eta + B_2 (\xi^2 + 3\eta^2)$$

Images of the test field were obtained at 3 different exposure stations A, B and C shown in Fig.4. Preliminary calibration tests were carried out for determining the parameters by use of these images. From these tests, it was found that the effect of 5 parameters $\lambda, \theta_1, \theta_3, B_1$ and B_2 was so small that these parameters could be disregarded.

New calibration computations were performed after disregarding the 5 parameters. Table 4 is the result. It is evident that each parameter is stable in magnitude through all over images and standard error σ_0 of an observation of image coordinates is less than $3.7 \mu\text{m}$. Therefore, the average values of Table 4 were used as the standard calibration values of the interior orientation elements. They are also described in Table 4.

5. Error of Object Space Coordinates Computed from Several Single Images

Table 4 Interior orientation elements obtained by 3 different images

Image	A	B	C	Average
$\xi_0 \times 10^3$ (mm)	-1221±13	-1215±24	1240±27	-1225
$\eta_0 \times 10^3$ (mm)	24±13	-10±28	-4±26	3
$c \times 10^3$ (mm)	46225±9	46260±21	46220±7	46.235
$\alpha \times 10^6$ (rad)	-4490±87	-4562±132	-4659±117	-4570
$A_1 \times 10^6$ (mm ⁻²)	-41.2±1.5	-51.2±6.3	-43.0±2.3	-45.1
$A_2 \times 10^9$ (mm ⁻⁴)	13.9±2.7	33.9±19.6	16.5±5.7	23.7
σ_0 (μm)	3.1	3.7	2.7	-

The images described in Section 4 were also used for estimating an accuracy of coordinate determination in the object space. Exterior orientation parameters of each individual image

were independently determined by applying a resection method of a single image. 4 stereoscopic pairs were thereafter selected to form the space models respectively, and object coordinates of 2 kind of points, control and check points, were computed. An example of the tests is shown below.

Only 8 control points were used for the exterior orientation and 5 points in those and other 10 check points were selected for estimating an error produced in each model. Some of the results are presented at Table 5, in which a relative depth error means an absolute value of a ratio of standard error of Z to Z. Table 5 shows that the error is fairly small throughout the tests³⁾, and increasing a base ratio, which results in convergent images, is effective for reducing an error.

6. Experiments of a Stereoscopic Measurement

All data described in the previous sections were the results which were obtained by measuring the targets on single images. Any result performed by a stereoscopic measurement is not yet presented. But the authors had succeeded in stereoscopic measurement by using a pair of rectified images, even in the case of converged image pair A-C. The measuring method will be explained with the aid of another test.

Table 5 Mean value of relative depth errors of targets

Model	Base ratio	(0/00) No. of points		
		5*)	10	Total
A-B	0.15~0.27	0.209	0.231	0.224
B-C	0.56~1.00	0.068	0.193	0.151
A-C	0.71~1.25	0.088	0.135	0.120
A-B-C	0.15~1.25	0.085	0.131	0.116

*) residual error at control points

6-1 Test Object

Fig.5 shows a different test performed in a room. 12 targets were pasted on a wall in the extent of 1.5 m width and 1.6 m height for a purpose of control points. The distance from the camera to the wall was 3.9 m. The distances between the camera stations and the objects were changed from exposure to exposure. Therefore, the principal distance of the camera was also changed so as to be suitable for good focussing.

6-2 Orientation

Measurement of coordinates of a center of a target was carried out on each image as described in Section 3. All control points signalized by targets were used for the relative and absolute orientation. Examples of the relative orientation elements and the estimated standard error of an observation of a target center in several models are shown in Table 6. Table 7 shows the mean value of a relative depth error in all 12 points described above. From the fact that the errors shown in Table 7 are similar in value to those shown in Table 5 and every error is reasonably small, it is recognized that the satisfactory results are obtained by both methods, the single-image orientation and the double-image orientation. But, in Table 7, it is not

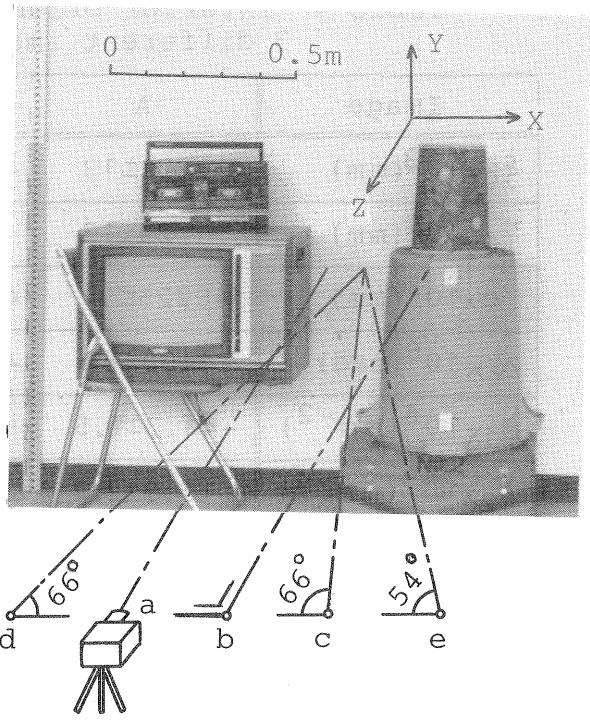


Fig.5 Test for stereoscopic measurements

Table 6 Result of the relative orientation of selected stereo pairs of images in Fig.5

Photo	a-b	b-c	b-e
ρ_1	1° 02' 13"	-1° 55' 08"	1° 50' 29"
κ_1	0° 02' 01"	0° 34' 47"	0° 25' 52"
ω_2	-0° 02' 21"	-0° 06' 19"	-0° 08' 24"
ρ_2	1° 12' 41"	24° 59' 09"	36° 33' 41"
κ_2	0° 08' 07"	0° 42' 59"	0° 38' 53"
σ_0	2.4 μm	1.7 μm	1.7 μm

Table 7 Mean Value of relative depth error of control points in the 2nd test

(0/00)

Model	a-b	b-c	b-e
B / Z	1/4	1/4	1/2
By original image (residual error)	0.094	0.164	0.094
By rectified image	0.165	0.287	0.241

evident that the error decreases as the base ratio B/Z increases as usually indicated.

6-3 Rectified Images

After performing the orientation, each original image was rectified digitally by use of the relative orientation elements from model to model so as to perceive a good stereoscopic impression. The bi-linear interpolation was employed for the digital image rectification.

A brief test concerning measuring accuracy was carried out with the aid of the rectified images. Location of the 12 control points indicated by the targets were again measured on each of the rectified images by the same method described in Section 3. And the locations of the control points were computed from these data. The error of the computed control points is also shown in Table 7 as to enable to compare with the residual error at the absolute orientation.

It is evident and natural that latter computed error in Table 7 is larger than the former residual error without exception. In spite of such fact, the latter error indicated is still reasonably small. This indicates that a considerably precise photogrammetry will be able to be performed by use of the system presented here.

6-4 Method of a Stereoscopic Measurement

Each one of a stereoscopic image pair was rectified and represented in a corresponding half part of the display. For a precise measurement, it may be effective in an usual photogrammetric work to view the rectified images through magnifying lenses. But in the case of viewing of the screen in the display, images should not be magnified through lenses because the pixel size on the screen appears too coarse to perceive a comfortable stereoscopic impression. The pixel size of the screen were 0.6 mm and the maximum pixel size to enable to feel a stereoscopic perception was estimated as 1.0 mm or so without viewing magnification from the authors' experience.

In order to perform a stereoscopically precise measurement, it is necessary to enlarge images on the screen because the minimum measuring unit of coordinates is pixel size (pitch). Only one method to realize it is to enlarge images and to view them, on the contrary, at a reduction ratio through lenses. For realizing this method, however, the fact that each half part of the screen contains only 256 pixels in width causes a bottleneck as follows. The pixel number of the screen was too small to perceive a good stereoscopic impression from the image pair enlarged more than 3 or 4 times. Considering these experiences, the enlargement ratio of original image was

Table 8 Test condition of stereoscopic measurements

Notation of a test	T1-1.5	T2-0.7
Digital enlargement factor	1	2
Optical magnification factor	1.5	0.7

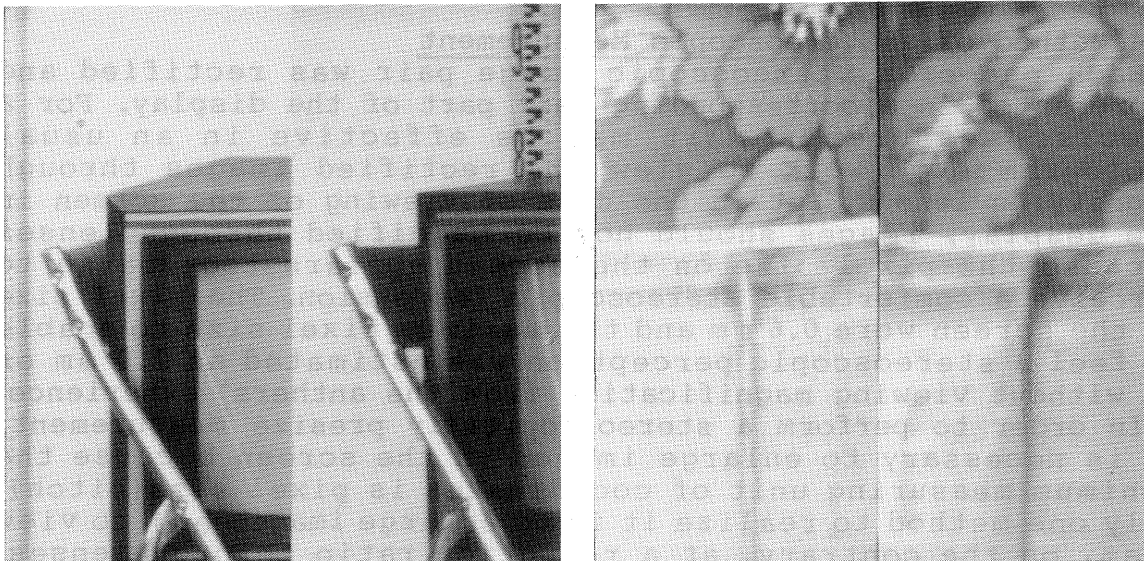
limited within 2 and as to the viewing magnification, on the other hand, the reduction ratio of 1~0.7 was adopted in this test. Table 8 indicates the notation and condition of the test. Fig.6 shows the examples of the image pair on the full screen.

There was another bottleneck in the system, which was caused by the fact that only one cursor was provided in the display unit. The cursor should be used for a measuring mark in this system. Therefore, a yellow square mark was selected as a cursor and another identical mark was produced in the image and represented on the screen. If the 2 marks were placed on the conjugate image points in question, a stereo model on which the mark was placed was perceived by the aid of a stereoscope. Even if such improvement had been performed, the new measuring mark could not still be moved on the screen. Owing to such limitation on mechanism, the stereoscopic measurement was carried out from point to point.

6-5 Test Measurements

Some results obtained from the test illustrated in Fig.5 are described below.

Graduation marks of a staff which was placed in the xy-plane were measured and the distance between graduations were



(a) TV, original scale

(b) upper part of a large cylinder, x3

Fig.6 Stereogram of Model b-e on the screen

Table 9 Distance measurement between graduations of a staff which is placed in the xy-plane (by the method T1-1.5)

		(mm)					
Distance in a staff		150	200	300	500	600	800
Distance measured in the model of	a-b			300.1	499.4		799.5
	b-c		200.3			598.9	800.1
	b-e	148.4		301.9			801.1

computed. The distances obtained from the test are in good agreement with those of staff as shown in Table 9. The image scale of the staff was 1 : 85. Consequently, an error 1 mm in the object space corresponds to an error 0.012 mm on the image.

The 2nd example is a measurement of front edges of a television frame. Corners and several points on the edges of the frame were measured stereoscopically in 3 models. An average of edge lines and the deviation from the average were computed from the measured coordinates. Fig.7 shows the deviation of the measured edges in 2 models. The accuracy is not good enough throughout the test. But, through a detail

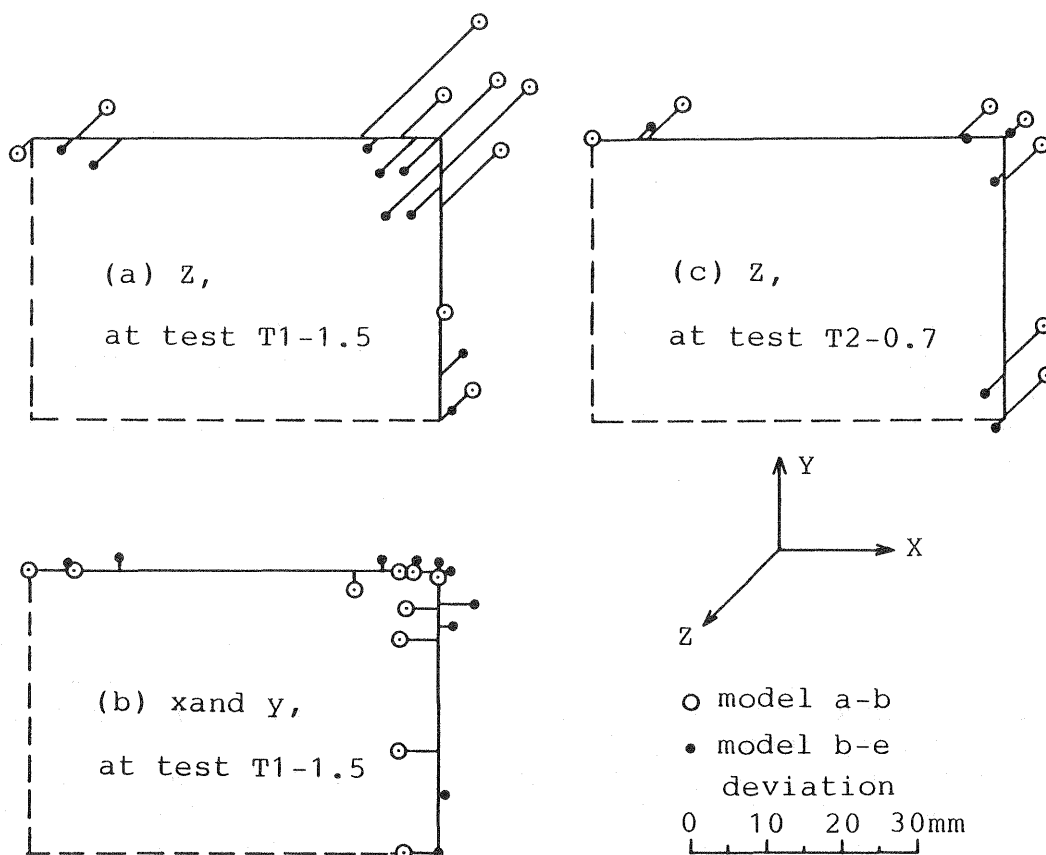


Fig.7 Deviation from the average edge lines

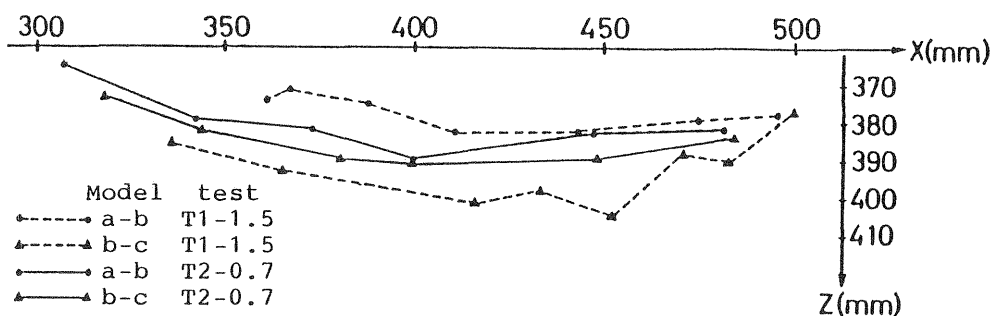


Fig.8 Horizontal section measured stereoscopically

inspection of Fig.7 (a) and (b) it seems that the deviation in model b-e is small and regular. It suggests that the accuracy in model b-e, which is formed from the remarkably convergent images, is best. Comparing Fig.7 (c) with (a), it is evident that the accuracy of Test T2-0.7 is better than that of Test T1-1.5.

As the 3rd example, a measurement of an upper part of a large cylindrical body shown in Fig.5 were carried out. Fig.8 shows the measured horizontal cross section in the 2 models with the 2 different methods of viewing. The error produced from the method T2-0.7 is distinctly smaller than that from the method T1-1.5 in this case, too.

7. Conclusions

Only a general-purpose computer system and standard computer peripherals were used, and any improvements of equipments were scarcely performed in this report. Nevertheless, fundamental works necessary to stereoscopic photogrammetry have been accomplished. The measuring accuracy in digital processing is fairly good in this test and also it is evident that a high accuracy will be achieved by improving a display unit. The most difficult task to be overcome will be to change a cursor currently used into a mechanism which is as convenient as a stereo-plotter.

The use of rectified images is advantageous for stereo matching⁴⁾. The stereo matching technique is important for automation of photogrammetry³⁾⁵⁾, but it is not dealt with in this report. Real time photogrammetry⁶⁾⁷⁾⁸⁾ is also excluded.

BIBLIOGRAPHY

- 1) J.Albertz and G.Koenig : A Digital Stereo photogrammetric System, Int. Archives of P & RS, Vol.25/2, pp.1-7(1984).
- 2) B.Kunji : Experiments in Digital Processing of Photogrammetric Images, ibed., pp.298-303(1984).
- 3) K.W.Wong : Close-Range Mapping with a Solid State Camera, Photogramm. Eng. and Remote Sensing, Vol.52, pp.67-74(1986).
- 4) S.Hattori, C.Mori and O.Uchida : A Coarse-to-Fine Correlation Algorithm Considering Occclusions, Int. Archives of P & RS, Vol.26, 3/2, pp.317-328.
- 5) H.Schewe : Automatishe photogrammetrische Karossrie-vermessung, Bildmessung und Luftbildwesen, 56 Jg., pp.16-23(1988).
- 6) K.W.Wong : Real Time Machine Vision System, The Canadian Surveyor, Vol.41, pp.173-180(1987).
- 7) A.W.Gruen and H.A.Beyer : Real Time Photogrammetry at the Digital Photogrammetric Station(DIPS) of ETH Zurich, ibed., pp.181-199(1987).
- 8) H.Haggrén : Real Time Photogrammetry as Used for Machine Vision Applications, ibid., pp.201-208(1987).